Molecular characterization of human Argonaute-containing ribonucleoprotein complexes and their bound target mRNAs

MARKUS LANDTHALER,[1] DIMOS GAIDATZIS,[2,3] ANDREA ROTHBALLER,[1] PO YU CHEN,[1] STEVEN JOSEPH SOLL,[1] LANA DINIC,[1] TOLULOPE OJO,[1] MARKUS HAFNER,[1] MIHAELA ZAVOLAN,[2] and THOMAS TUSCHL[1]

[1]Laboratory of RNA Molecular Biology, Howard Hughes Medical Institute, The Rockefeller University, New York, New York 10065, USA
[2]Swiss Institute of Bioinformatics, Biozentrum, University of Basel, CH-4056 Basel, Switzerland

ABSTRACT

microRNAs (miRNAs) regulate the expression of mRNAs in animals and plants through miRNA-containing ribonucleoprotein particles (RNPs). At the core of these miRNA silencing effector complexes are the Argonaute (AGO) proteins that bind miRNAs and mediate target mRNA recognition. We generated HEK293 cell lines stably expressing epitope-tagged human AGO proteins and other RNA silencing-related proteins and used these cells to purify miRNA-containing RNPs. Mass spectrometric analyses of the proteins associated with different AGO proteins revealed a common set of helicases and mRNA-binding proteins, among them the three trinucleotide repeat containing proteins 6 (TNRC6A,-B,-C). mRNA microarray analyses of these miRNA-associated RNPs revealed that AGO and TNRC6 proteins bind highly similar sets of transcripts enriched in binding sites for highly expressed endogenous miRNAs, indicating that the TNRC6 proteins are a component of the mRNA-targeting miRNA silencing complex. Together with the very similar proteomic composition of each AGO complex, this result suggests substantial functional redundancy within families of human AGO and TNRC6 proteins. Our results further demonstrate that we have developed an effective biochemical approach to identify physiologically relevant human miRNA targets.

Keywords: microRNA; Argonaute; GW182/TNRC6; microRNA targets; immunoprecipitation

INTRODUCTION

miRNAs comprise a large family of evolutionary conserved small regulatory RNAs that have important regulatory functions in a wide array of biological processes, including developmental timing, cell differentiation, cell proliferation, apoptosis, and patterning of the nervous system (Ambros 2004; Jones-Rhoades et al. 2006; Bushati and Cohen 2007).

miRNA biogenesis has been reviewed in detail (Lee et al. 2006a; Chapman and Carrington 2007). Briefly, miRNAs are processed from long primary RNA polymerase II transcripts (pri-miRNAs) by the RNase III Drosha and the associated double-stranded RNA-binding protein DGCR8 into hairpin pre-miRNAs (Denli et al. 2004; Gregory et al. 2004; Han et al. 2004, 2006; Landthaler et al. 2004). The pre-miRNAs are exported to the cytoplasm by exportin-5 (Yi et al. 2003; Lund et al. 2004) and are further processed by the RNase III nuclease DICER (Bernstein et al. 2001; Grishok et al. 2001; Hutvágner et al. 2001; Ketting et al. 2001). Typically, only one strand of the miRNA duplex is incorporated into the miRNA silencing effector protein (miRNPs) complexes (Khvorova et al. 2003; Schwarz et al. 2003). The mature miRNA then guides miRNPs to messenger RNAs (mRNAs).

The recognition of mRNAs by miRNPs results in mRNA cleavage of targeted transcripts that are perfectly complementary to the miRNA (Hutvágner and Zamore 2002; Yekta et al. 2004; Barth et al. 2008) and inhibition of translation in case of limited base-pairing interactions between the 5′-end of the miRNA and complementary sequences in the 3′-untranslated regions (UTRs) of the target mRNAs (Wightman et al. 1993). Experimental

[3]**Present address:** Friedrich-Miescher Institute for Biomedical Research, CH-4058 Basel, Switzerland.

Reprint requests to: Thomas Tuschl, Laboratory of RNA Molecular Biology, Howard Hughes Medical Institute, The Rockefeller University, New York, NY 10065, USA; e-mail: ttuschl@rockefeller.edu; fax: (212) 327-7652; or Mihaela Zavolan, Swiss Institute of Bioinformatics, Biozentrum, University of Basel, CH-4056 Basel, Switzerland; e-mail: Mihaela.Zavolan@unibas.ch.

Article published online ahead of print. Article and publication date are at http://www.rnajournal.org/cgi/doi/10.1261/rna.1351608.

evidence suggests that the inhibition of protein synthesis mediated by miRNPs takes place at the stage of translational initiation (Humphreys et al. 2005; Pillai et al. 2005; Thermann and Hentze 2007), as well as during the later elongation step (Olsen and Ambros 1999; Seggerson et al. 2002; Zeng et al. 2002; Petersen et al. 2006). In addition, miRNAs can also induce degradation of mRNA targets despite imperfect miRNA–mRNA base pairing (Bagga et al. 2005; Jing et al. 2005; Krutzfeldt et al. 2005; Lim et al. 2005; Rehwinkel et al. 2005; Giraldez et al. 2006; Schmitter et al. 2006; Wu et al. 2006; Grimson et al. 2007; Linsley et al. 2007; Rodriguez et al. 2007).

In animal cells, miRNAs recognize their target mRNAs through base-pairing interactions between 6 and 8 nucleotides (nt) at the 5′ end of the miRNA, the so-called ''seed,'' and complementary nucleotides in the 3′ UTR of mRNAs. Computational methods to predict miRNA binding sites in several organisms mostly rely on the interaction of the miRNA seed region with its target mRNA 3′ UTR and evolutionary conservation of the target site (John et al. 2004; Grun et al. 2005; Krek et al. 2005; Lewis et al. 2005; Gaidatzis et al. 2007; Grimson et al. 2007). Different experimental approaches have been used to identify miRNA targets and to study the physiological interactions of miRNAs and target mRNAs (Krutzfeldt et al. 2005; Lim et al. 2005; Rehwinkel et al. 2006; Schmitter et al. 2006; Vinther et al. 2006; Beitzinger et al. 2007; Easow et al. 2007; Karginov et al. 2007; Orom and Lund 2007; Zhang et al. 2007; Zhao et al. 2007; Baek et al. 2008; Hendrickson et al. 2008; Selbach et al. 2008).

Biochemical and genetic studies have shown that Argonaute (AGO) proteins are the core component of miRNP silencing complexes (Hammond et al. 2001; Martinez et al. 2002; Mourelatos et al. 2002; for reviews, see Meister and Tuschl 2004; Patel et al. 2006; Tolia and Joshua-Tor 2007). AGO proteins share a conserved PAZ and PIWI domain, and both domains are involved in the interaction with small RNAs (Song et al. 2003; Yan et al. 2003; Lingel et al. 2004; Ma et al. 2004). Structural studies further revealed that the PIWI domain adopts an RNase H-like fold, which forms the catalytic center of the AGO endonuclease in the RNA-induced silencing complex (Song et al. 2004; Ma et al. 2005; Parker et al. 2005).

A number of proteins were found to be associated with AGO proteins and the miRNP complexes (for reviewed, see Peters and Meister 2007). More recently, biochemical purifications of human EIF2C1/AGO1 and EIF2C2/AGO2 revealed additional factors, including helicases, heterogeneous nuclear ribonucleoproteins, mRNA-binding proteins and proteins involved in RNA metabolism (Hock et al. 2007). Several of these proteins function in the biogenesis and activity of miRNAs. DICER and the double-stranded RNA binding proteins, TARBP2 and PRKRA/PACT, are involved in processing of the miRNA precursor (Chendrimada et al. 2005; Haase et al. 2005; Lee et al. 2006b). RNA helicase A (DHX9) interacts with RNA-induced silencing complex (RISC) in human cells and functions in RISC loading (Robb and Rana 2007). TNRC6A/GW182 and TNRC6B, markers of mRNA-degrading cytoplasmic processing bodies (P- or GW-bodies), are required for RNA interference in human cells (Jakymiw et al. 2005; Liu et al. 2005; Meister et al. 2005). The TNRC6 proteins seem to function downstream of Argonaute in the process of mRNA degradation with the final steps likely to occur in P-bodies (Behm-Ansmant et al. 2006). Another P-body component, the helicase RCK/DDX6, is also required for translation regulation by miRNAs highlighting the importance of the cytoplasmic P-body structures in RNA silencing (Chu and Rana 2006).

We performed a comprehensive biochemical analysis to understand the molecular composition of the human RNA silencing machinery by proteomic and ribonomic profiling of the human AGO RNPs. We observed a common set of protein interactors for EIF2C1,-2,-3,-4, including DICER, TNRC6A,-B,-C (or GW182 proteins), heat-shock proteins, helicases, and various mRNA-binding proteins. The mRNA profiles of immunoprecipitates of the four AGO proteins and their associated TRNC6 proteins were strikingly similar and characterized by the enrichment of transcripts with seed sequence complementarity to expressed miRNAs. The high similarity of AGO- and TNRC6-immunopurified mRNAs suggests a substantial degree of redundancy in the regulatory function within the AGO and TNRC6 protein families, and further provides evidence that these proteins are components of the miRNA-containing mRNA-targeting complexes.

RESULTS

Proteomic analysis of human argonaute protein interactors

To characterize the molecular composition of human EIF2C1/AGO1 through EIF2C4/AGO4 (collectively referred to as AGO proteins) containing protein complexes, we generated HEK293 cells stably expressing FLAG/HA-tagged AGO proteins. FLAG/HA-AGO protein complexes were affinity purified from HEK293 total cell extracts by incubation with anti-FLAG agarose beads. The immunoprecipitated FLAG–protein complexes were eluted using FLAG peptide, followed by a second immunoprecipitation (IP) using anti-HA magnetic beads. The immunoprecipitated proteins were then separated by SDS-PAGE (Supplemental Fig. 1), excised, and identified by mass spectrometry (MS). Table 1 lists the names of the identified proteins in FLAG/HA-EIF2C1,-2,-3,-4 IPs. Surprisingly, all four AGO proteins coimmunoprecipitated a highly similar set of proteins. We identified the previously described interactors DICER, MOV10, TNRC6A, and TNRC6B (as well as the paralogous TNRC6C as a new interactor). Reciprocal purifications

TABLE 1. Summary of proteins identified by double-affinity purifications

Identified protein[a]	Accession number	MW	EIF2C1 IP	EIF2C2 IP	EIF2C3 IP	EIF2C4 IP	DICER1 IP	TNRC6A IP	TNRC6B IP
DICER1	NP_803187	218552	13/10[b]	1/2	1/2	3/4	49/72	–	–
TNRC6A	NP_055309	210167	16/15	7/9	6/7	3/7	–	5/5	–
TNRC6B	NP_055903	182557	21/26	19/27	16/16	12/13	–	–	13/17
TNRC6C	NP_061869	175834	18/22	13/19	6/8	13/14	–	–	–
MOV10	NP_066014	113541	17/17	16/12	27/26	20/15	–	–	–
EIF2C1	NP_036331	97084	70/47	–	18/11[c]	–	7/5	32/21	23/16
EIF2C2	NP_036286	97077	17/10[c]	73/50	9/4[c]	–	15/7	45/29	27/19
EIF2C3	NP_079128	97230	27/17[c]	–	49/33	12/10[c]	–		–
EIF2C4	NP_060099	96966	–	10/8[c]	–	55/35	–		–
TARBP2	NP_599150	38908	–	–	–	–	46/11		–
PRKRA	NP_003681	34273	–	–	–	–	32/8		–
HSP90AA1	NP_005339	84543	15/11	31/20	32/20	25/14	–	16/13	9/3
HSP90AB1	NP_031381	83133	10/8	32/22	31/20	11/8	–	25/16	6/5
HSPA1A	NP_005336	69907	41/26	35/21	21/11	–	9/6	48/23	14/9
HSPA2	NP_068814	69890	–	–	8/4	–	–		–
HSPA5	NP_005338	72202	–	10/5	–	–	–	28/14	–
HSPA6	NP_002146	70897	–	–	–	–	8/6		–
HSPA8	NP_006588	70767	34/21	–	–	18/10	–	43/23	–
HSPA9	NP_004125	68288	12/7	7/5	5/3	–	–		5/3
HSPD1	NP_002147	60924	14/6	–	–	–	–		–
PABPC1	NP_002559	70540	23/14	33/18	37/19	29/17	–	16/8	17/10
PABPC4	NP_003810	70652	18/8	24/13	26/15	19/10	–	9/4	–
HNRNPAB	NP_112556	35837	–	–	13/4	6/2	–	–	–
HNRNPA2B1	NP_002128		16/5	–	–	19/5	–	–	–
HNRNPA3	NP_919223	39464	–	–	18/3	12/3	–	–	–
HNRNPC	NP_001070910	33539	–	24/8	24/7	–	29/8	7/2	5/2
HNRNPD	NP_112738	38303	–	–	9/3	6/2	–	–	–
HNRNPF	NP_004957	45541	–	13/5	10/3	10/3	–	–	–
HNRNPH1	NP_005511	49099	10/4	19/6	18/6	17/5	14/5	20/7	–
HNRNPK	NP_002131	50897	7/3	4/2	–	11/4	–	–	–
HNRNPL	NP_001524	64002	11/5	6/4	–	9/4	–	19/9	–
HNRNPM	NP_005959.2	77385	13/8	11/10	15/8	15/9	14/10	–	5/4
HNRNPR	NP_005817	70812	–	–	8/5	11/7	–	–	–
HNRNPU	NP_114032	90454	19/11	3/2	12/8	12/8	–	–	–
RBMX	NP_002130	42201	–	–	9/2	–	–	–	–
SYNCRIP	NP_006363	69502	–	–	8/4	–	–	4/2	–
DHX9	NP_001348	140828	10/11	–	1/2	6/5	–	6/7	–
DDX17	NP_006377	80142	6/4	3/2	14/7	8/5	–	5/3	2/2
DDX5	NP_004387	69017	–	–	–	8/3	–	7/4	1/1
DDX3X	NP_001347	73113	3/2	–	–	–	–	12/7	–
XRCC5	NP_066964	82574	–	6/5	3/2	–	–	–	–
XRCC6	NP_001460	69712	–	9/5	–	–	–	–	–
IGF2BP1	NP_006537	63350	6/4	14/7	23/10	17/7	–	18/7	–
IGF2BP2	NP_006539	65991	5/3	2/1	20/7	8/3	–	4/2	–
IGF2BP3	NP_006538	63574	12/7	13/7	22/11	18/7	–	–	–
FUBP3	NP_003925	61510	–	5/3	3/2	–	–	–	–
ZNF326	NP_892021	65523	–	–	7/2	–	–	–	–
RBM14	NP_006319	69361	12/6	3/2	10/6	8/4	–	3/2	–
YBX1	NP_004550	35793	28/6	9/3	12/3	17/4	–	–	–
ELAVL1	NP_001410	35961	–	–	14/3	23/5	–	–	–
RALY	NP_057951	32332	–	–	11/3	13/4	–	–	–
SSB	NP_003133	46706	19/7	2/1	–	–	–	–	–
CSDA	NP_003642	39929	15/6	–	–	–	–	–	–
NCL	NP_005372	76484		–	–	–	–	–	–
ILF2	NP_004506	42931	10/2	–	12/5	16/5	22/7	–	–
ILF3	NP_036350	95208	–	–	12/7	5/3	6/5	–	–
STAU1	NP_059346	54803	–	–	–	–	13/6	–	–

(*continued*)

TABLE 1. *Continued*

Identified protein[a]	Accession number	MW	EIF2C1 IP	EIF2C2 IP	EIF2C3 IP	EIF2C4 IP	DICER1 IP	TNRC6A IP	TNRC6B IP
STAU2	NP_055208	52638	–	–	–	–	8/4	–	–
TP53	NP_000537	43522	48/14	–	–	16/5	–	11/3	–
EEF2	NP_001952	95207	10/4	–	–	–	–	29/9	–
EEF1A1	NP_001393	50010	24/8	17/9	–	–	–	–	–
ADAR	NP_001102	135837	–	–	–	–	17/17	–	–
GNL2	NP_037417	83524	–	–	–	–	32/22	–	–
RPL[d]			+	+	+	+	+	+	+
RPS[d]			+	+	+	+	–	+	+

[a]AGO and DICER IPs were performed twice, whereas TNRC6A and TNRC6B IPs were performed once. In the case of AGO and DICER purifications, only proteins identified in both IPs are indicated.
[b]Numbers indicate percentage coverage of protein sequence/number of peptides identified.
[c]Identified by single unique peptide and peptides shared with other AGO proteins.
[d]Presence (+) and absence (–) of identified proteins belonging to large (RLP) and small ribosomal subunits (RLS) in purifications are indicated.

using tagged DICER, TNRC6A, and TNRC6B-expressing cells lines confirm these interactions (Table 1). In addition IPs of FLAG/HA-DICER coprecipitated among other proteins the know interactors TARBP2 and PRKRA/PACT (Chendrimada et al. 2005; Haase et al. 2005; Lee et al. 2006b).

Furthermore, we encountered a number of additional proteins in AGO IPs. These copurified proteins fell within several functional groups. The largest group included the mRNA-binding proteins, in particular the heterologous nuclear ribonucleoproteins: HNRNPAB, HNRNPC, HNRNPD, HNRNPF, HNRNPH1, HNRNPK, HNRNPL, HNRNPM, SYNCRIP/HNRPQ, HNRNPR, and HNRNPU. In addition, we detected several mRNA-binding proteins with functions in mRNA transport, stabilization and translation, most prominently IGF2BP1–IGF2BP3, YBX1, ELAVL1, FUBP3, and RALY. Moreover, the polyadenylate binding proteins 1 and 4 (PABPC1 and PABPC4) were present in the IPs. In addition the RNA helicases DDX5, DDX17, and DHX9, but not DDX6, which is required for miRNA function (Chu and Rana 2006), were identified as well as a series of 40S and 60S ribosomal proteins.

The interaction of selected proteins with the AGO proteins was confirmed by co-IP experiments (Fig. 1). Cells stably expressing FLAG/HA-EIF2C1 were transfected with plasmids encoding the myc-tagged version of several proteins that were identified by MS. Extracts from transfected cells were immunoprecipitated with anti-FLAG agarose and FLAG eluted. The eluted proteins were separated by SDS-PAGE, blotted, and probed with an anti-myc antibody. The myc-tagged proteins EIF2C1, EIF2C2, DICER, TNRC6C, MOV10, DDX17, PABPC4, YBX1, IGF2BP3, and ELAVL1 could be coimmunoprecipitated, whereas the mRNA-binding protein QKI, which was not identified in the MS analysis, but is expressed in HEK293 cells (data not shown), could not be detected. Treatment of the lysate with RNase T1 prior to the IP abolished the interaction with most proteins except DICER and TNRC6C, suggesting that the interactions between FLAG/HA-EIF2C1 and the other myc-tagged proteins were RNA mediated.

AGO proteins associate with ribosomes

miRNAs and miRNA-repressed mRNAs, as well as AGO proteins, have been described to be associated with polysomes

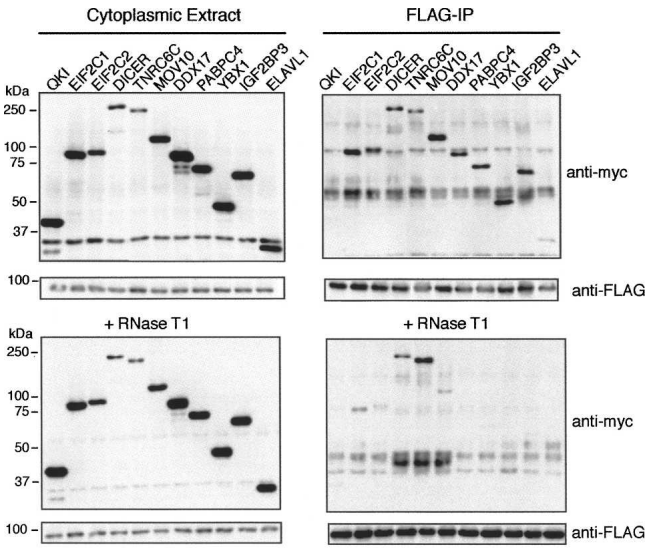

FIGURE 1. Proteins identified by mass spectrometry interact with EIF2C1. HEK293 cells stably expressing FLAG/HA-EIF2C1 were transfected with constructs encoding myc-tagged variants of the proteins identified by MS. Transfected cells were lysed and cytoplasmic extracts prepared in the absence or presence (+RNase T1) of ribonuclease T1. FLAG/HA-EIF2C1 was immunoprecipitated using anti-FLAG beads and eluted from the beads using FLAG peptide. Cell extracts and FLAG-eluted proteins (FLAG-IP) were separated by SDS-PAGE, blotted, and probed with anti-HA and anti-myc antibodies.

(Olsen and Ambros 1999; Seggerson et al. 2002; Kim et al. 2004; Nelson et al. 2004; Maroney et al. 2006; Nottrott et al. 2006; Balzer and Moss 2007; Vasudevan and Steitz 2007). We re-examined the distribution of EIF2C2, exemplary for the AGO family, using polysome gradients. Cytoplasmic extracts of FLAG/HA-tagged cells were prepared and fractionated on sucrose gradients (Fig. 2). The absorbance profiles at 254 nm showed a pattern of ribosomes of exponentially growing cells with ribosomal subunits, monosomes, and polysomes. The protein fractions of the gradient were separated by SDS-PAGE, blotted, and probed with an antibody against ribosomal protein L7 (RPL7), a component of the 80S monosome and the 60S large subunit, to identify the ribosome-containing fractions. Consistent with previous findings (Maroney et al. 2006; Nottrott et al. 2006; Balzer and Moss 2007), probing the blot with an anti-HA antibody indicated the presence of FLAG/HA-EIF2C2 throughout the gradient, including the the polysomal fractions. In polysome gradients of a cellular extract that was prepared in the presence of 30 mM EDTA, to dissociate the polysome into the ribosomal subunits and monosomes, FLAG/HA-EIF2C2 shifted from the denser fractions to the lighter fractions of the gradient, suggesting that EIF2C2 cofractionates with polysomes as observed previously for miRNAs (Maroney et al. 2006; Nottrott et al. 2006).

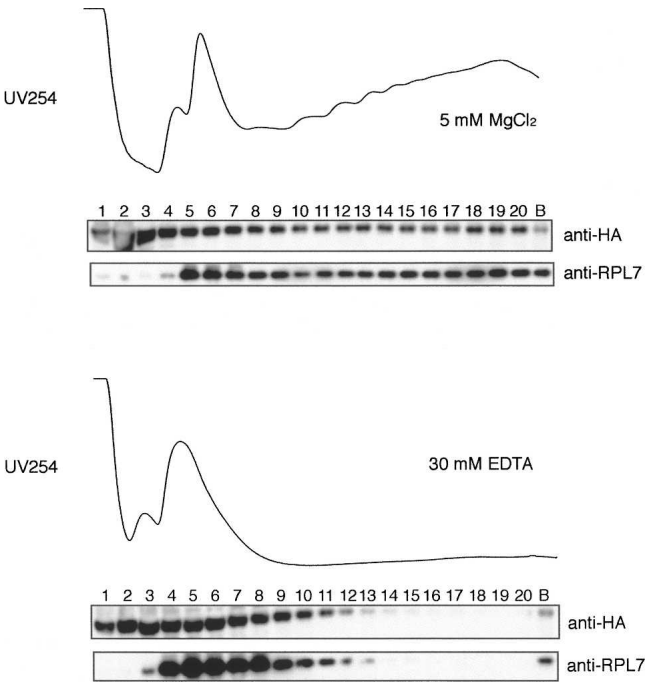

FIGURE 2. EIF2C2 is associated with polysomes in HEK293 cells. Cytoplasmic extracts were prepared by cell lysis with buffer containing 5 mM $MgCl_2$ or 30 mM EDTA, centrifuged through sucrose gradient, and fractionated. Proteins of each fraction were TCA-precipitated and equal aliquots were separated by SDS-PAGE, blotted, and probed with antibodies as indicated. Absorbance of fractions at 254 nm is shown.

Next, we immunoprecipitated FLAG/HA-EIF2C2 with anti-FLAG beads from cytoplasmic extracts prepared with 2 mM EDTA to partially dissociate the polysomes. The precipitated protein complexes were eluted with FLAG peptide and loaded on a 10%–45% sucrose gradient and fractionated by centrifugation. Probing for FLAG/HA-EIF2C2 with an anti-HA antibody indicated that the epitope-tagged AGO protein was present in at least three major complexes, which we designated complexes I, II, and III (Fig. 3A), similar to observations made by Hock et al. (2007). The coimmunoprecipitated ribonuclease DICER sedimented with complex I, likely representing the RISC loading complex previously described (Pellino et al. 2005). Interestingly, in complex III we were able to detect the small and large ribosomal subunit proteins, RPS6 and RPL7, respectively. The presence of both of these proteins suggests that FLAG/HA-EIF2C2 is associated with the 80S ribosome, whereas complex II constitutes the small ribosomal subunit. Northern hybridization using a probe for miR-16, a highly abundant miRNA in HEK293 cells, showed the association of this miRNA with each of the three complexes (Fig. 3B).

miRNA target identification by AGO immunoprecipitation

To confirm that the characterized complexes indeed represent miRNPs involved in silencing, we developed a method to characterize the mRNAs present in these complexes. To identify the mRNAs associated with FLAG/HA-tagged AGO protein complexes, we isolated total RNA from the FLAG-immunoprecipitates (IPs) and performed an mRNA microarray analysis. IPs of AGO-containing protein complexes was confirmed by Western analysis (Supplemental Fig. 2A) and by Northern hybridization for miR-16 (Supplemental Fig. 2B).

mRNA profiles of the cleared lysates prior to the IPs were highly similar with correlation coefficient values of 0.94–0.99. The high similarities of the expression profiles between cells expressing various tagged proteins indicate that the expression of the tagged AGO proteins had little effect on mRNA expression profiles. The normalized mRNA profiles of IPs and cleared lysates were compared to determine the degree of enrichment of each individual transcript in the IP versus the lysate. The distribution of the fold changes of the enrichment and underrepresention of transcripts that were immunopurified in different experiments are summarized in Supplemental Figure 3.

For a subset of experiments, we also compared the immunoprecipitated mRNAs with the mRNA profile of the supernatants after the IP. Since contrasts generated by comparing the profile of the IP mRNA versus lysate mRNA or supernatant mRNA were qualitatively similar, only the IP/lysate contrasts were used for further analyses.

To determine whether or not different AGO proteins bind to the same mRNA transcripts, we selected the top

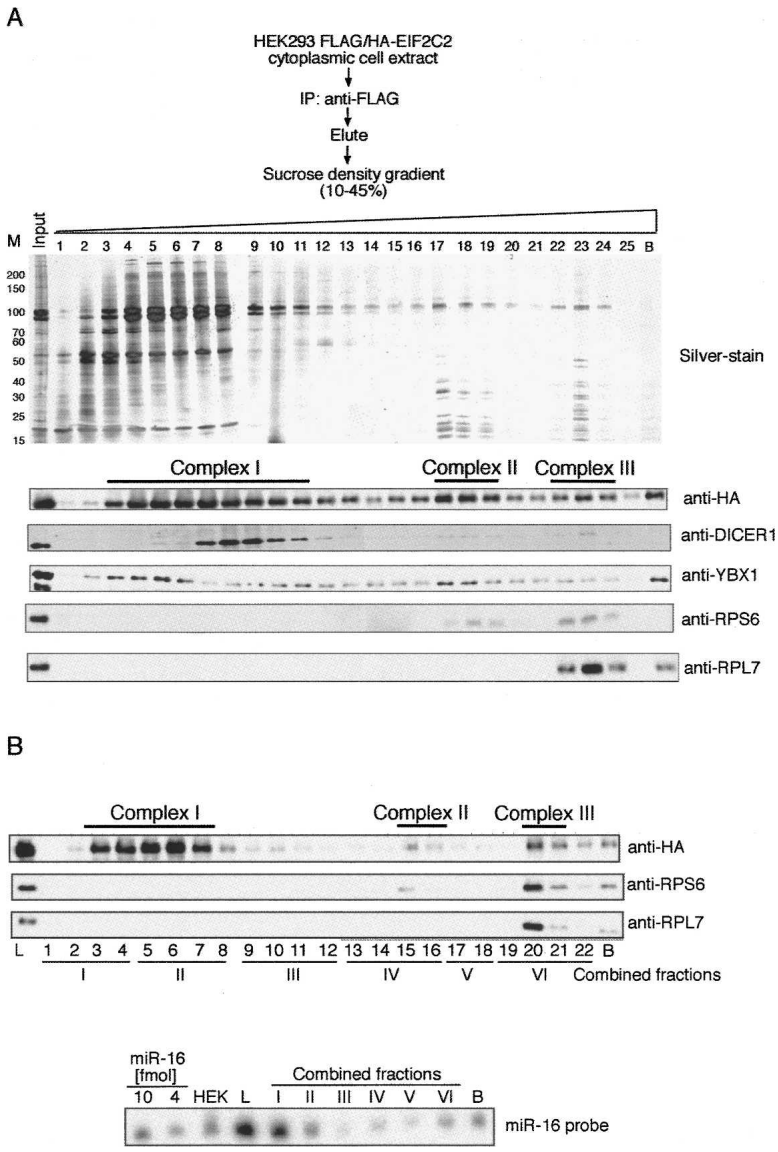

FIGURE 3. EIF2C2 is associated with ribosomes. (*A*) FLAG/HA-EIF2C2 was immunoprecipitated from a cytoplasmic extract prepared with lysis buffer containing 2 mM EDTA. The epitope-tagged protein was eluted using FLAG peptide and separated on a 10%–45% sucrose gradient for 8.5 h. Proteins of each fraction were TCA precipitated and separated by SDS-PAGE (silver-stained gel is shown on *top*). Western analysis of the separated fractions was performed using antibodies as indicated. (*B*) miR-16 is associated with three FLAG/HA-EIF2C2-containing complexes. FLAG/HA-EIF2C2 was purified and displayed on a sucrose gradient as described in *A*. The distribution of FLAG/HA-EIF2C2 in the gradient was examined by Western analysis using an anti-HA antibody and compared with the presence of RPS6 and RPL7 with antibodies against these ribosomal proteins. RNA was extracted from the material loaded on to the gradient (L), and each fraction of the gradient, pooled as indicated, separated by 15% denaturing PAGE, blotted, and probed for miRNA miR-16. A total of 20 μg of HEK293 cellular RNA (HEK) was loaded along with 10 and 4 fmol of synthetic miR-16 as control.

2.5% immunoprecipitated transcripts in each individual experiment indicated in Figure 4A, and used the union of these transcripts to perform two-dimensional hierarchical clustering. We found a striking similarity between the mRNAs purified by anti-FLAG-agarose IPs of epitope-tagged EIF2C1,-2,-3,-4. This set of enriched transcripts was a result of specific binding of mRNAs directly or indirectly to the immunoprecipitated proteins, since it was obtained independently of the antibody or bead matrix used in these experiments. IPs of the FLAG/HA-tagged EIF2C2 expressing cells using an anti-FLAG, an anti-HA, and a monoclonal antibody against EIF2C2 bound by Protein G magnetic beads, as well as an IP of FLAG/HA-QKI-expressing cells using the anti-EIF2C2 antibody, immunopurified a set of transcripts highly similar to that obtained from FLAG-agarose IPs. The high similarity of the mRNAs bound by EIF2C1,-2,-3,-4 is mirrored by the striking resemblance in the proteomic composition, suggesting that AGO proteins likely have redundant regulatory functions.

To demonstrate that the mRNP complexes isolated by the FLAG/HA-EIF2C1,-2,-3,-4 IPs indeed contained mRNAs targeted by miRNAs, the 3′ UTRs of the enriched transcripts were scanned for the presence of sequences complementary to the seed sequences of miRNAs expressed in HEK293. For this purpose, we clustered the seed sequences into seed groups (SG) according to the expression level of the corresponding miRNA family members in HEK293 cells (Table 2). SG1 comprises the seed sequences of the five most highly expressed miRNA families (S1–S5), whereas SG2 and SG3 contain the miRNA families that rank S6–S10 and S11–S15, respectively (Table 2). The density of seed-complementary motifs in the 3′ UTR of the enriched mRNAs was compared with the density of these motifs in a set of size-matched 3′ UTRs that were not enriched in the IP. A value of 1 indicates that the density of miRNA seed-complementary motifs is the same between immunoprecipitated transcripts and mRNAs that are expressed but not immunoprecipitated (control set). By performing repeated random selections of control transcripts, we obtained an estimate of the variance in the calculated enrichment in seed-complementary sites. Moreover, we compared the enrichment obtained for the most highly expressed miRNAs to that calculated for random subsets of miRNAs that were not expressed in HEK293 cells (NSG1–NSG3;

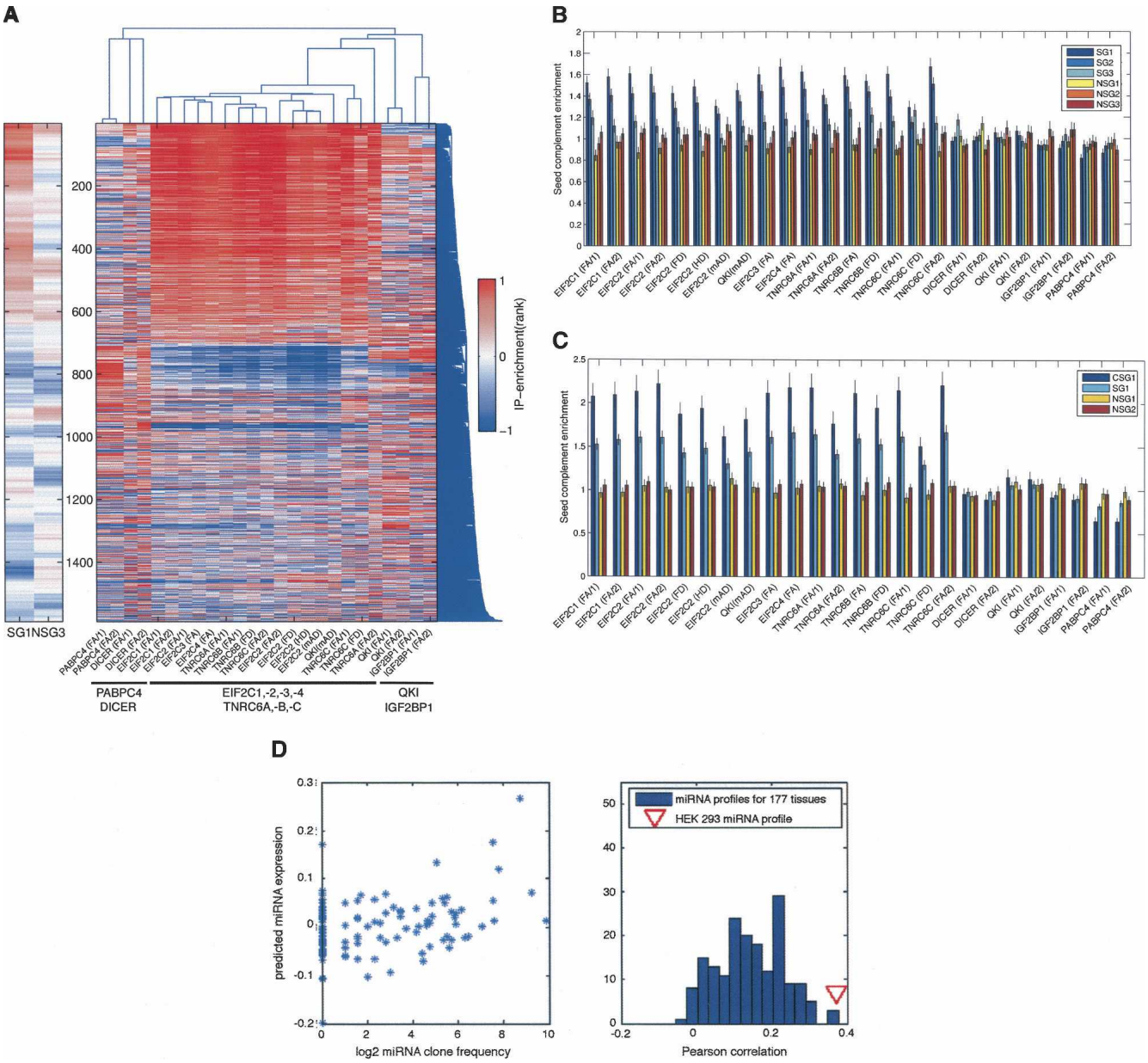

FIGURE 4. AGO and TNRC6 proteins immunopurify a similar set of transcripts enriched for sequences complementary to miRNA seeds (*A*) Two-dimensonal hierarchical clustering for the enriched transcripts in IPs. IPs were performed from extracts of cells stably expressing the FLAG/HA-tagged protein as indicated using anti-FLAG agarose beads (FA) or Protein G Dynabeads bound anti-FLAG (FD), anti-HA (HD), and monoclonal anti-Ago2 (mAD) antibodies with the number of the biological replicates indicated in parentheses. Immunoprecipitated transcripts were defined as transcripts that have a high rank (top 2.5%) in each of the indicated IP experiments. Number of transcripts is shown on the *left*. The *left* panel additionally shows seed enrichment (SG1, NSG3) for the transcripts clustered in the *right* panel. (*B*) Seed complement enrichment for HEK293 miRNAs in immunoprecipitated transcripts compared with transcripts that were not enriched in the IP. The top 5% most enriched transcripts and random subsets containing the same number of not enriched transcripts obtained from each IPs were scanned for the presence of sequences complementary to the three HEK293 seed groups (SG1–SG3) and the control nonseed group 1–3 (NSG1–NSG3), representing control seed groups of miRNAs not expressed in HEK293 cells. IPs are described in *A*. (*C*) Enrichment for conserved seed complements for HEK293 miRNAs in immunoprecipitated transcripts. CSG1 (conserved seed group 1) refers to conserved seed hits of the top five expressed miRNAs. SG1 refers to seed hits of the top five expressed miRNA seed groups without conservation information, and NSG1 and NSG2 represent control miRNA seed groups. (*D*) Predicting miRNA profiles from AGO-immunoprecipitated transcripts. In the *left* panel a linear regression model was used to infer the activities of each miRNA seed family (nucleotides 1–8, 133 seed families in total; see Landgraf et al. 2007) based on the representation of transcripts carrying seed matches in AGO-IP. Seed families whose reverse complements are frequent in the immunoprecipitated transcripts receive high activity scores, whereas seed families that do not correlate with the IP data receive low scores. The *right* panel shows a histogram of the Pearson correlation coefficients resulting from the comparison of the miRNA "activity" predicted by the linear model with each of the measured miRNA expression profiles. The profiles that went into the construction of the histogram are from data of the 177 samples of Landgraf et al. (2007) and the HEK293 profile determined by 454 sequencing in this study (red triangle).

TABLE 2. Expression of HEK293 miRNA seed families

Seed family	Seed sequence	Representative miRNA	Total clone counts	Family members (454 clone counts)	miRNA sequences
S1	UAGCAGCA	hsa-miR-16	923 (22.4%)	hsa-miR-16(652)	UAGCAGCACGUAAAUAUUGGCG
				hsa-miR-15a(175)	UAGCAGCACAUAAUGGUUUGUG
				hsa-miR-15b(90)	UAGCAGCACAUCAUGGUUUACA
				hsa-miR-195(6)	UAGCAGCACAGAAAUAUUGGC
S2	UGUAAACA	hsa-miR-30e-5p	598 (14.5%)	hsa-miR-30e-5p(230)	UGUAAACAUCCUUGACUGGA
				hsa-miR-30c(186)	UGUAAACAUCCUACACUCUCAGC
				hsa-miR-30a-5p(99.5)	UGUAAACAUCCUCGACUGGAAG
				hsa-miR-30b(73)	UGUAAACAUCCUACACUCAGCU
				hsa-miR-30d(9.5)	UGUAAACAUCCCCGACUGGAAG
S3	UGUGCAAA	hsa-miR-19a	418 (10.1%)	hsa-miR-19b(230)	UGUGCAAAUCCAUGCAAAACUGA
				hsa-miR-19a(188)	UGUGCAAAUCUAUGCAAAACUGA
S4	UAUUGCAC	hsa-miR-32	220 (5.3%)	hsa-miR-32(194)	UAUUGCACAUUACUAAGUUGC
				hsa-miR-92(26)	UAUUGCACUUGUCCCGGCCUG
S5	CAUUGCAC	hsa-miR-25	185 (4.5%)	hsa-miR-25(185)	CAUUGCACUUGUCUCGGUCUGA
S6	UAAAGUGC	hsa-miR-20a	184 (4.5%)	hsa-miR-20a(117.33)	UAAAGUGCUUAUAGUGCAGGUAG
				hsa-miR-106b(67)	UAAAGUGCUGACAGUGCAGAU
S7	UAGCUUAU	hsa-miR-21	132 (3.2%)	hsa-miR-21(132)	UAGCUUAUCAGACUGAUGUUGA
S8	CAAAGUGC	hsa-miR-17-5p	98 (2.4%)	hsa-miR-17-5p(97.33)	CAAAGUGCUUACAGUGCAGGUAGU
				hsa-miR-20b(1)	CAAAGUGCUCAUAGUGCAGGUAG
S9	AAAGUGCU	hsa-miR-93	92 (2.3%)	hsa-miR-93(92)	AAAGUGCUGUUCGUGCAGGUAG
S10	UUUGGCAA	hsa-miR-182	85 (2.1%)	hsa-miR-182(85)	UUUGGCAAUGGUAGAACUCACA
S11	CAGCAGCA	hsa-miR-424	78 (1.9%)	hsa-miR-424/322(70)	CAGCAGCAAUUCAUGUUUUGAA
				hsa-miR-497(8)	CAGCAGCACACUGUGGUUUGU
S12	UCAGUGCA	hsa-miR-148a	70 (1.7%)	hsa-miR-148a (50)	UCAGUGCACUACAGAACUUUGU
				hsa-miR-148b (16)	UCAGUGCAUCACAGAACUUUGU
				hsa-miR-152 (4)	UCAGUGCAUGACAGAACUUGG
S13	UUCACAGU	hsa-miR-27b	58 (1.4%)	hsa-miR-27b (58)	UUCACAGUGGCUAAGUUCUGC
					UUCACAGUGGCUAAGUUCCGC
S14	UAUGGCAC	hsa-miR-183	58 (1.4%)	hsa-miR-183 (58)	UAUGGCACUGGUAGAAUUCACU
S15	CAGUGCAA	hsa-miR-130a	57 (1.4%)	hsa-miR-301b (27)	CAGUGCAAUGAUAUUGUCAAAGC
				hsa-miR-130b (23)	CAGUGCAAUGAUGAAAGGGCAU
				hsa-miR-301a (4)	CAGUGCAAUAGUAUUGUCAAAGC
				hsa-miR-130a (3)	CAGUGCAAUGUUAAAAGGGCAU

see Supplemental Table 1). Figure 4B shows that the immunopurified mRNAs are enriched in sites complementary to SG1 through SG3, respectively, whereas no enrichment could be observed for control seed groups (NSG1–NSG3). The seed complement enrichment generally decreased with the relative expression of the corresponding miRNAs.

To provide further evidence that the immunoprecipitated transcripts are indeed functional miRNA targets, we computed the enrichment of conserved miRNA seed complements using a method for estimating the probability that a miRNA binding site is under evolutionary selection (Gaidatzis et al. 2007). We found a significantly stronger enrichment in these sites, indicating that the IP captures functional miRNA targets, which were selected during evolution (Fig. 4C).

Yet another indication that our approach identifies bona fide miRNA targets is provided by a linear regression model, with which we attempt to predict the transcript enrichment in the IP in terms of the number of miRNA seed matches in the 3′ UTR of transcripts and a vector of miRNA-dependent weights, representing the concentrations of miRNAs in a cell. By fitting these miRNA-specific weights we derive a relative miRNA expression profile in the cell. More precisely, given that the prediction of miRNA target sites is based solely on the seed sequence of miRNAs, we cannot distinguish between different miRNAs carrying the same seed sequence; therefore, what we predict is the seed expression profile. We compared the predicted profile with the 177 profiles obtained from different tissues (Landgraf et al. 2007), and found that the predicted profile most strongly correlates with the experimentally determined HEK293 miRNA profile (Fig. 4D). Thus, the AGO-immunoprecipitated mRNAs enable one to reconstruct, to some extent, the miRNA expression profile of the sample. Figure 4D additionally shows a positive correlation coefficient between the predicted HEK293 miRNA expression profile and the profiles obtained experimentally from other types of cells, likely due to the presence of a subset of miRNAs with broad tissue distribution.

miRNA transfection and immunopurification of miR-122 targets

Another method to define miRNA targets relied on miRNA transfection experiments to identify miRNA-regulated mRNAs by measuring the reduction of transcripts caused by the addition of the exogenous miRNA (Lim et al. 2005; Grimson et al. 2007). To provide additional experimental support for our approach to identify miRNA-targeted mRNAs, we transfected FLAG/HA-EIF2C2-expressing cells with miR-122, a liver-specific miRNA, and compared the cellular RNA and RNA isolated from FLAG IPs with that of mock-transfected cells, similar to experiments performed previously (Karginov et al. 2007; Hendrickson et al. 2008). Northern analysis showed that miR-122 was transfected and recovered in the immunoprecipitate (Fig. 5A). Furthermore, mRNAs immunoprecipitated from the miR-122-transfected cells exhibit a strong enrichment in miR-122 seed-complementary sites (Fig. 5B), whereas the transcripts immunoprecipitated from mock-transfected cells were enriched only in sequences complementary to the HEK293 endogenous SG1–SG3, but not for the miR-122 seed.

In summary, these analyses demonstrated that our IP protocol was able to capture targets of both endogenously expressed, as well as transfected miRNAs, and that the immunoprecipitated mRNA population reflects the miRNA population present in the cell.

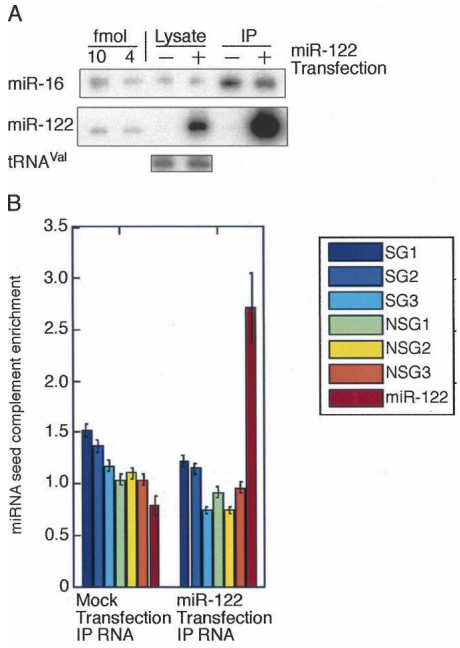

FIGURE 5. miR-122 transfection and immunoprecipitation of miR-122 mRNA targets. (*A*) Cells stably expressing FLAG/HA-EIF2C2 were mock transfected and transfected with a miR-122 duplex. Fifteen hours after transfection cells were lysed and the epitope-tagged protein was immunoprecipitated from cytoplasmic extracts with anti-FLAG antibody. RNA was extracted from the cleared cell lysate and the IP. RNA was separated by 15% denaturing PAGE and probed for miR-16 and miR-122. A total of 10 and 4 fmol of synthetic miR-16 and miR-122, respectively, were loaded as standards. The miR-16 blot was reprobed with an oligonucleotide antisense to valine tRNA to ensure equal loading of lysate RNA. (*B*) Analysis of enriched mRNAs in Ago-IP. The EIF2C2-IP-enriched transcripts were scanned for the presence of sequences complementary to the three HEK293 seed groups (SG1–SG3), the control nonseed groups 1–3 (NSG1–NSG3), and the miR-122 seed in the 3′ UTR. The first and second bar group show the enrichment of complements in immunoprecipitated transcripts of the mock-transfected and mir-122-transfected cells, respectively.

AGO and TNRC6 protein IPs enrich similar mRNAs with miRNA seed complements

Next, we compared the mRNA populations obtained by IP of proteins associated with AGO, including DICER, TNRC6A-C, IGF2BP1, PABPC4, and QKI as control (summarized in Supplemental Table 2). We found a striking similarity between the mRNAs purified by anti-FLAG-agarose IPs of epitope-tagged EIF2C1,-2,-3,-4 and TNRC6A-C (Fig. 4A), indicating that AGO and TNRC6 proteins are part of identical or largely overlapping mRNP complexes. This conclusion was also supported by the observation that the interaction between AGO and TNRC6 proteins is RNase resistant (Fig. 1). Furthermore, a set of about 600 transcripts was shown to be reproducibly associated with EIF2C1,-2,-3,-4 and TNRC6A,-B,-C proteins (Fig. 4A).

AGO and DICER IPs had some mRNAs in common. However, the overlap was far less significant than the one observed between AGO and the TNRC6-immunoprecipitated transcripts (Supplemental Fig. 4), although we could show a stable protein–protein interaction between DICER and EIF2C1 (Fig. 1).

The sets of transcripts immunoprecipitated by the IGF2BP and QKI proteins overlapped to some extend with the sets of transcripts immunoprecipitated by AGO and TNRC6. IGF2BP1 was identified in the double affinity purifications of AGO proteins and was shown to interact with AGO proteins in co-IP experiments in an RNA-dependent manner (data not shown).

In contrast, the PABPC4-IPed RNA did not reveal any significant overlap, although an RNA-mediated interaction with EIF2C1 could be observed (Fig. 1). In fact, some of the most enriched transcripts in PABPC4-immunoprecipitated are only present at low levels in the AGO-IPs (Supplemental Fig. 4).

As expected, TNRC6-immunoprecipitated transcripts showed a clear enrichment in miRNA seed-complementary sites analogous to AGO-immunoprecipitated transcripts (Fig. 4B,C), whereas no seed enrichment was observed for mRNAs in DICER, IGF2BP1, QKI, and PABPC4 IPs. These results indicated that AGO and TNRC6 protein-containing mRNP complexes associated with miRNA targets and are components of the miRNP silencing effector complexes. The seed enrichment analysis further suggested that neither QKI nor IGF2BP1 are part of the miRNA effector complexes defined by AGO and TNRC6 proteins. Interestingly,

the PABPC4-IPed transcripts showed a significant reduction in evolutionarily selected seed-complementary sites, suggesting that the poly(A) tails of miRNA-targeted mRNAs might be less accessible for the epitope-tagged PABPC4, consistent with the observation of shorter poly(A) tails on miRNA-targeted mRNAs (Behm-Ansmant et al. 2006; Giraldez et al. 2006; Wu et al. 2006; Wakiyama et al. 2007).

Experimental validation of miRNA targets

To verify experimentally if the enriched mRNAs are indeed negatively regulated by HEK293 miRNAs, we generated dual luciferase reporter constructs containing the 3′ UTRs of 16 of the 20 most enriched mRNAs in EIF2C1,-2,-3,-4 IPs (Supplemental Table 2). We were unable to amplify the other four unusually long 3′ UTRs. The luciferase activity increased reproducibly for 14 of the 16 reporter constructs when cotransfected with a pool of antisense 2′-*O*-methyl oligoribonucleotides to block the activity of the 12 most highly expressed HEK293 miRNAs, compared with a transfection with an unspecific 2′-*O*-methyl control oligoribonucleotide (Fig. 6). The binding of the respective mRNAs to AGO protein complexes and repression by miRNAs confirmed that the IPed mRNAs are regulated by miRNAs in vivo.

DISCUSSION

In this present study, we provide the results of a comprehensive proteomic and ribonomic profiling study to elucidate the protein, the small RNA, and target mRNA composition of the four human AGO protein and other RNA silencing-related protein complexes.

Proteomic analysis

In contrast to other studies, our survey included the proteomic characterization of all four human AGO family members (EIF2C1,-2,-3,-4) and revealed that all of them associate with a similar set of helicases, hnRNPs, and mRNA-binding proteins, as well as DICER and members of the TNRC6 protein family. The composition of EIF2C1 and EIF2C2 RNP complexes showed a significant overlap with interactors recently identified (Hock et al. 2007). We were unable to detect several proteins that were identified by a single peptide in the MS analysis by Hock et al. (2007). Among these were several DEAD/DEXH helicases (DDX39, DDX46, DHX36) and the RNA-binding protein RBM4, which was shown to be involved in miRNA-mediated regulation (Hock et al. 2007). This suggests that these proteins might only be transiently associated with AGO protein-containing complexes.

Of the other identified interactors, DICER and the members of the TNRC6 protein family have been shown to be essential in miRNA precursor processing (Bernstein et al. 2001; Grishok et al. 2001; Hutvágner et al. 2001) and miRNA-mediated translational repression and mRNA decay, respectively (Jakymiw et al. 2005; Liu et al. 2005; Meister et al. 2005; Rehwinkel et al. 2005; Behm-Ansmant et al. 2006; Eulalio et al. 2008). We provide further biochemical evidence that these proteins form stable complexes with AGO proteins.

DICER cosediments with EIF2C2 in the lighter density complex I, which likely represents the RISC loading complex (RLC). Our analysis of the DICER immunoprecipitated mRNAs suggests that DICER and its associated proteins are not part of the miRNA effector complexes, since the DICER-enriched transcripts shared no significant similarity to AGO-immunoprecipitated miRNA targets. Recent in vitro reconstitution experiments of the human RLC indicated that EIF2C2 dissociates from this complex once it is loaded with miRNAs, suggesting that AGO proteins disengage from the RLC before targeting mRNAs (MacRae et al. 2008).

We showed previously that TNRC6B interacts with EIF2C1 and EIF2C2, and that the protein localizes to P-bodies and is required for miRNA-mediated mRNA cleavage

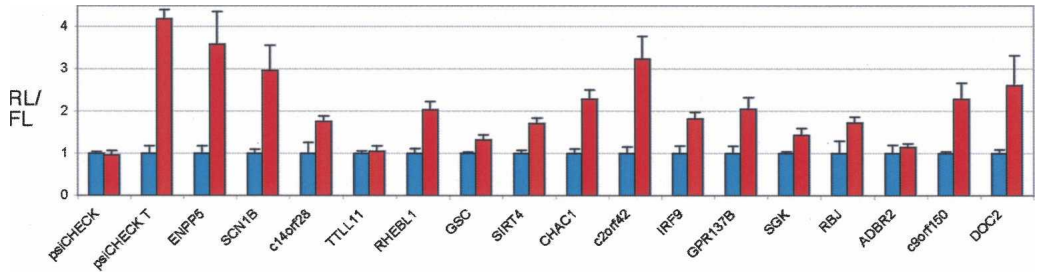

FIGURE 6. miRNA-mediated repression of 3′ UTRs fused to luciferase reporter genes. Luciferase activity from HEK293 cells cotransfected with each reporter/control psiCHECK construct and 2′-*O*-methyl oligoribonucleotides antisense to 12 HEK293 miRNAs (red bars) was normalized to that from cotransfection of each reporter construct with 2′-*O*-methyl oligoribonucleotide antisense to *Drosophila* miRNA bantam (blue bars). Transfection of parental psiCHECK vector without inserted 3′ UTR (psiCHECK) and 3′ UTR with two artificial binding sites each for miR-16 and miR-196b (psiCHECK T) are indicated. Error bars represent standard deviation of experiment performed with six replicates. Normalized Renilla luciferase (RL) versus firefly luciferase (FL) activities are indicated.

(Meister et al. 2005). Here, we provide evidence that the human TNRC6 proteins interact stably with the mRNA-bound miRNP effector complexes, since miRNA-targeted mRNAs are highly enriched in TNRC6 proteins complexes. Zhang et al. (2007) made similar observations for AIN-1 and AIN-2, two *C. elegans* proteins homologous to the human TNRC6 protein family. As observed for the two TNRC6 proteins in the nematode, the mRNAs immunoprecipitated by the three human TNRC6 members overlapped extensively, supporting the idea that the different proteins may act redundantly and regulate a highly similar set of mRNAs.

Our proteomic analyses further revealed that AGO-containing complexes (as well as TNRC6-containing complexes) contained components of the translational machinery. We identified ribosomal proteins belonging to the small and large subunits, whereas other proteins commonly associated with the P-bodies, like proteins of the decapping machinery (Jakymiw et al. 2005; Liu et al. 2005; Meister et al. 2005) and the helicase DDX6 (Chu and Rana 2006), were not detected. In addition, we observed cosedimentation of EIF2C2 with polysomes, and association with the small subunit of the ribosome (complex II) as well as the 80S ribosome (complex III). Our results contrast previous observations (Hock et al. 2007), which described sedimentation coefficients for AGO mRNP complexes II and III of ~19S and 25–30S, respectively.

The observed localization of EIF2C2 to polysomes is consistent with several previous studies suggesting that translation is regulated by miRNPs at a step after initiation. In *C. elegans*, miRNA-targeted mRNAs were discovered in polysomes (Olsen and Ambros 1999; Seggerson et al. 2002). Additional studies demonstrated that siRNAs and miRNAs associate with polysomes (Kim et al. 2004; Nelson et al. 2004; Maroney et al. 2006; Nottrott et al. 2006; Petersen et al. 2006). Furthermore, the *D. melanogaster* 80S RISC complex was found to contain ribosomes (Pham et al. 2004).

miRNA target identification

The isolation of mRNAs bound to EIF2C1,-2,-3,-4 and TNRC6A,-B,-C-containing protein complexes resulted in the identification of a highly similar set of transcripts, whose 3′ UTRs are enriched for sequences that are complementary to miRNA seed sequences (positions 1–8).

Our biochemical approach identified miRNA targets based on the association of these transcripts with human AGO and TNRC6 protein complexes. These results are consistent with the previously described physical interactions and functional relationship of TNRC6A and B with AGO proteins (Jakymiw et al. 2005; Liu et al. 2005; Meister et al. 2005; Wakiyama et al. 2007; Eulalio et al. 2008). TNRC6C is a novel component of this interaction network. Moreover, the nearly identical sets of mRNAs coimmunoprecipitated by the different AGO and TNRC6 proteins, respectively, suggest a high degree of redundancy between the members of each protein family with regard to their mRNA targets, and may also exhibit redundancy on a functional level. The targeting redundancy of human AGO proteins is reflected in their ability to bind identical miRNAs (Liu et al. 2004; Meister et al. 2004).

Our approach focused on the identification of physiologically relevant targets of endogenously expressed miRNAs in human cells, as similar efforts have in *Drosophila* Schneider S2 cells and in *C. elegans* (Easow et al. 2007; Zhang et al. 2007). Other IP approaches in human cells focused on the identification of mRNA targets of single, transfected miRNAs that are bound to EIF2C2 (Karginov et al. 2007; Hendrickson et al. 2008).

We identified about 600 transcripts to be regulated in HEK293 cells, a number that is substantially lower than the number of predicted targets for miRNAs expressed in HEK293 cells and the about 1200 and 2500 enriched transcripts recently identified by IP of EIF2C2 in HEK293 cells (Karginov et al. 2007; Hendrickson et al. 2008). Our seed complement density analysis revealed that only the highly expressed miRNAs leave detectable signatures in the immunoprecipitated mRNAs, suggesting that the highly expressed miRNAs have a biologically significant function or are amenable to experimental analysis of miRNA regulation in biological systems.

The dual luciferase reporter assay results demonstrated that the absolute degree of regulation mediated by miRNAs varies between 1.5- and 3.5-fold. The magnitude of regulation is likely dependent on the number of miRNP effector complexes associated with the target mRNA, since the level of repression achieved is dependent on both the amount of mRNA and the number of available miRNP complexes (Doench and Sharp 2004). In addition, miRNPs function in the context of other post-transcriptional regulatory networks. AGO and TNRC6 protein complexes contain a number of mRNA-binding proteins (mRBPs) with functions in mRNA transport, stabilization, and translation, such as IGF2BP1 (Yisraeli 2005). Recent observations indicate that the interplay of miRNPs and *trans*-acting mRBPs regulate the abundance of mRNAs and the rate of their translation in response to stress and environmental signals (Leung and Sharp 2007). The following examples illustrate the competition or synergism of various mRNA-binding factors and the modular architecture of post-transcriptional regulatory elements. HuR/ELAVL1, an AU-rich element-binding protein also identified in our AGO IPs, relieves a miRNA-induced inhibition of translation in cells subjected to different stress conditions (Bhattacharyya et al. 2006). The RNA-binding protein Dnd1 inhibits miRNA access to target mRNA (Kedde et al. 2007). Furthermore, EIF2C2 and fragile X mental retardation-related protein 1 were shown to activate the

translation of tumor necrosis factor-α upon cell cycle arrest (Vasudevan et al. 2007).

miRNA target predictions have been valuable tools for defining putative miRNA-regulated transcripts. However, prediction methods have several kinds of limitations. First, the rules for base-pairing of the miRNA seed with the evolutionary conserved target transcript sites were shown not to be exclusive indicators of miRNA/mRNA interactions (Krutzfeldt et al. 2005; Didiano and Hobert 2006). Annotations of mRNA sequences, in particular 3′ UTR sequences, might be incomplete or inaccurate (Rajewsky 2006). Prediction methods have mainly focused on target identification in 3′ UTR sequences and the impact of potential binding sites in other locations of the transcript remains to be determined. Finally, the information about expression levels and patterns of miRNAs and mRNAs were not taken into consideration in any of the computational predictions. Experimental data sets that allow for the testing of these predictions have recently been reported (Baek et al. 2008; Selbach et al. 2008).

The first experimental approaches to identify miRNA-regulated mRNAs on a transcriptome-wide level involved recording the stability of transcripts upon miRNA expression and inhibition (Krutzfeldt et al. 2005; Lim et al. 2005). These approaches have their limitations, as only target mRNAs were revealed that show changes in steady-state levels. Furthermore, these methods, as well as recently reported quantitative proteomic approaches (Baek et al. 2008; Selbach et al. 2008), rely on the introduction of miRNAs or miRNA-inhibitory ''antagomirs,'' which could have an unintended impact on physiological regulatory interactions between miRNAs and their target mRNAs and are limited to the study of the altered miRNA.

Our experimental approach, as well as other IP-based methods, which identify miRNA-associated transcripts independent of the effect on mRNA stability, (Beitzinger et al. 2007; Easow et al. 2007; Karginov et al. 2007; Zhang et al. 2007; Hendrickson et al. 2008) allow the discovery of miRNA-regulated mRNAs without prior knowledge of the rules of interaction between miRNA and target mRNAs and the evolutionary conservation of this regulatory relationship. In our case, the target identification by IP indicates the feasibility of the method to define physiologically relevant miRNA-regulated transcripts without overexpression or depletion of miRNAs. We expect that a more detailed analysis of these experimentally determined miRNA-targeted transcripts will provide further insight into the sequence and structural features that affect the regulation of these transcripts in their natural environment, as well as the combinatorial regulation by different miRNA families.

In summary, we have shown that IPs of AGO and TNRC6 proteins resulted in an enrichment of miRNA targets, which correlated with the miRNA expression profile in HEK293 cells and was only detectable for the 15 most strongly expressed miRNA seed families. Furthermore, our IP experiments using a monoclonal antibody against human EIF2C2 demonstrate the possibility to identify miRNA-targeted mRNAs in human cells and tissues, which allows one to uncover the physiological miRNA regulatory networks in humans. Ultimately, additional biochemical approaches are necessary to determine the exact in vivo binding sites of mRBPs and miRNPs, thus establishing a comprehensive high-resolution map of the mRNA-RBP/miRNP interaction landscape. Defining this ''messenger ribonucleoprotein code'' and its sequence requirements will provide a better understanding of the mechanisms mediating post-transcriptional control of gene expression and the complexity of this regulatory network.

MATERIAL AND METHODS

Plasmids and antibodies

Plasmids and antibodies are described in the Supplemental Materials. Plasmids are made available through Addgene (www.addgene.com).

Double-affinity purification of FLAG/HA-tagged protein complexes

Cells were harvested from 8–10 L of suspension culture by centrifugation, washed in PBS, and frozen after resuspension of the cell pellet (about 15 mL) in an equal volume of freezing buffer (50 mM HEPES-KOH at pH 7.4, 1 mM EGTA, 1 mM $MgCl_2$, 100 mM KCl, and 10% glycerol). Frozen cells were pulverized with a mortar and lysed in 3 mL/g frozen cell suspension (75 mM HEPES-KOH at pH 7.4, 1.5 mM EGTA, 1.5 mM $MgCl_2$, 150 mM KCl, and 15% glycerol, 0.075% NP-40, EDTA-free Protease Inhibitor Cocktail [Roche]) by sonication. The cell lysate was cleared by centrifugation at 25.000*g* for 45 min at 4°C. IP was performed for 3 h at 4°C using the FLAG-specific monoclonal antibody M2 covalently coupled to agarose beads (Sigma). The immunoprecipitate was washed six times in Wash300 buffer (50 mM HEPES-KOH at pH 7.4, 1 mM EGTA, 1 mM $MgCl_2$, 3 mM KCl, and 10% glycerol, 0.05% NP-40, 1 mM DTT, EDTA-free Protease Inhibitor Cocktail) and twice in Wash100 buffer (as Wash300 buffer but with 100 mM KCl). FLAG-tagged proteins were eluted by addition of 500 μg of synthetic 1×FLAG peptide per 1 mL of Wash100 buffer, followed by rotation for 1 h at 4°C. FLAG-eluted proteins were further immunoprecipitated using μMACS HA-beads (Miltenyi) for 1 h and eluted in 1× SDS-loading buffer. Eluted proteins were separated on 4%–12% NUPAGE SDS-PAGE (Invitrogen) and stained with Gelcode Blue (Pierce).

Mass spectrometry

Protein bands were excised from stained SDS–polyacrylamide gels, washed, and digested with trypsin. Tryptic peptides were isolated and liquid chromatography–tandem mass spectrometry analyses were performed on a Nano HPLC coupled to an ion-trap (ThermoElectron Finnigan LTQ) mass spectrometer. Peptide fragment ion spectra were searched against the nonredundant protein database for matches using MASCOT (Matrix Science).

Transfection and co-IP

For miR-122 transfection experiments, FLAG/HA-EIF2C2 cells were transfected with miR-122 duplex or mock transfected using Lipofectamine RNAiMAX as described by manufacturer.

For transient transfection of cells, stably expressing FLAG/HA-EIF2C1, pDESTmyc constructs were delivered using Lipofectamine 2000 as described by the manufacturer. Cells were lysed in 50 mM HEPES-KOH (pH 7.4), 150 mM KCl, 2 mM EDTA, 0.5 mM DTT, 1 mM NaF, and 0.5% NP-40. The cell lysate was cleared. For RNase treatment, lysate was incubated for 20 min at room temperature with RNase T1 at 1 U/μL. IP was performed as described above with ANTI-FLAG M2-agarose beads. The immunoprecipitate was washed 3× in Wash300 buffer and 2× in Wash100 buffer. FLAG-tagged proteins were eluted by addition 1×FLAG peptide. Eluted proteins were loaded separated by SDS-PAGE, blotted, and probed with anti-HA and anti-myc antibodies. Primary antibodies were detected with HRP-conjugated secondary antibodies using the ECL Plus Western Blotting Detection System (Amersham).

Sucrose density fractionation

Cells were washed with ice-cold PBS, lysed in 10 mM HEPES-KOH (pH 7.4), 150 mM KCl, 5 mM $MgCl_2$ or 30 mM EDTA, and 0.5% NP-40, and centrifuged for 5 min to pellet the nuclei. Polysome fractionations of 200 μL of cell extract were performed in 12 mL of gradients from 10%–45% (w/v) sucrose in 10 mM HEPES-KOH (pH 7.4), 150 mM KCl supplemented with either 5 mM $MgCl_2$ or 30 mM EDTA. Lysates were separated by centrifugation at 38,000 rpm for 1.5 h in a SW41 rotor at 4°C. FLAG-peptide-eluted protein complexes from immunoprecipitates were separated by centrifugation at 38,000 rpm for 8.5 h in a SW41 rotor at 4°C in 10%–45% (w/v) sucrose gradient in 10 mM HEPES (pH 7.4), 150 mM KCl, and 5 mM $MgCl_2$.

RNA isolation from cell lysate and FLAG-protein immunoprecipitates

About 15 mL of cell pellet were lysed in three cell pellet volumes of 50 mM HEPES-KOH (pH 7.4), 150 mM KCl, 2 mM EDTA, 0.5 mM DTT, 1 mM NaF, and 0.5% NP-40. RNA from the lysate was isolated by adding 3 vol of RNA extraction solution (4 M guanidinium isothiocyanate, 25 mM sodium citrate, 0.5% N-lauroylsarcosinate, 50 mM β-mercaptoethanol, and 50% acidic phenol) and 0.2 volumes of chloroform. RNA was ethanol-precipitated from the aqueous phase. FLAG/HA-tagged or endogenous protein was immunoprecipitated with anti-FLAG M2 agarose beads or antibody-bound Protein G Dynabeads (Invitrogen). Beads were washed three times with 50 mM HEPES-KOH (pH 7.4), 300 mM KCl, 2 mM EDTA, 0.5 mM DTT, 1 mM NaF, and 0.05% NP-40. RNA isolation from immunoprecipitated RNPs was performed as described previously (Meister et al. 2004). RNA for microarray analysis was further purified using RNeasy mini spin columns (QIAGEN). Quality of RNA was assessed using the Agilent Bioanalyzer.

Microarray analysis

A total of 2 μg of purified total RNA from HEK293 cell lysate or from immunoprecipitated RNPs was used in the One-Cycle Eukaryotic Target Labeling Assay (Affymetrix) according to the manufacturer's protocol. Biotinylated cRNA targets were cleaned up, fragmented, and hybridized to Human Genome U133 Plus 2.0 Array (Affymetrix).

miRNA Northern hybridization

miRNA Northern analysis was performed as described previously (Landthaler et al. 2004).

Dual luciferase assay

HEK293 cells were cotransfected in 96-well format (40.000 cells/well) with 100 ng of the respective psiCHECK vector and a total of 120 pmoles of a pool of 2′-*O*-methyl oligoribonucleotides (anti-miR-15a, anti-miR-16, anti-miR-17, anti-miR-18, anti-miR-19a, anti-miR-19b, anti-miR-20a, anti-miR-20b, anti-miR-32, anti-mir-92, anti-miR-93, and anti-mir-196b) antisense to the respective miRNA or 120 pmoles of 2′-*O*-methyl oligoribonucleotide antisense to the *Drosophila*-specific miRNA bantam with Lipofectamine 2000 (Invitrogen). Cells were lysed in 1×Passive Lysis Buffer (Promega) 15 h after transfection and analyzed using the Dual-Luciferase Reporter System (Promega) as described by the manufacturer on a BIO-TEK Clarity 96-well plate reader with double injectors.

Computational analysis of microarray data

The probe intensities were normalized for all the microarray experiments using the bioconductor (see http://www.bioconductor.org and Gentleman et al. (2004) and gcRMA software (Wu et al. 2004). To quantify effects based on the frequency of seed-complementary sites in the 3′ UTRs, we selected, for each gene measured by the microarray, the transcript with median 3′ UTR length. This data set consisted of 14,658 transcripts. From all of the probe sets corresponding unambiguously to a given gene, we selected the one that responded best (exhibited the highest variance) across a large number of experiments performed on the Affymetrix platform that we used. This probe set was used to monitor the per-transcript expression level across our experiments. Based on the transcript expression levels computed this way, we calculated the Pearson correlation coefficient of mRNA expression between pairs of experiments.

Selection of transcripts for the analysis of target spectra of different RNA-binding proteins

In order to compare the target spectra of different RNA-binding proteins, we extracted from each sample the top 2.5% most enriched transcripts in a particular IP of a specific protein relative to lysate. This amounts to 195 transcripts per sample from a total of 7820, for which we had expression evidence in HEK293 cells. We used the union of these transcripts (1589) to perform hierarchical clustering. The clustering results are rather insensitive to variations in the number of transcripts that we select from each sample, but larger transcript sets are more difficult to visualize.

Construction of miRNA seed groups

The miRNA profile of HEK293 cells was first determined as described in the Supplemental Materials.. We used this profile to

rank the miRNA expression. To improve the reliability of our statistics of miRNA target site enrichment, we performed this analysis for one group of miRNAs at a time as follows. One of the most reliable indicators of a miRNA target site is the perfect complementarity to the 5′ end of the miRNA (Lewis et al. 2005). We therefore divided miRNAs sets based on the sequence they carry at positions 1–8. For each of these sets, we computed the total expression in HEK293 by summing the counts of all miRNAs within a set. Such a sequence set typically contains paralogous miRNA genes. We then ranked the expression of these sets, and constructed groups of five sequence sets at a time, starting from the highest to the lowest expressed sequence set. We called these groups SG1, SG2, SG3, etc. For reference, we also created random groups of five sequence sets (NSG1–NSG3) that were not expressed in HEK293 cells (see Supplemental Table 1).

Enrichment of miRNA target sites in transcripts that co-IP with RNA-binding proteins

We assessed the enrichment in miRNA target sites of the set of transcripts bound by a given RNA-binding protein as follows. We selected the top 5% transcripts that were IPed with the given RNA-binding protein. For each miRNA seed family (nucleotides 1–8), we determined the density (sites/nucleotides) of seed (1–7, 2–8, and 1–8) complementary sites in the given set of transcripts. This quantity was compared with the density of the same motifs in a random subset of transcripts of the same size, which were not enriched in the IP (background set). The background transcripts where chosen such that their fold change in the IP compared with lysate was in the 25%–75% range. By repeating the procedure of selecting background subsets of transcripts 100 times, we obtained means and standard deviations for motif enrichment in the various samples.

Enrichment of evolutionarily selected target sites in transcripts that coimmunoprecipitate with mRNA-binding proteins

The algorithm described by Gaidatzis et al. (2007) was used to obtain for each putative miRNA target site a posterior probability that the site is under selection. Then, we applied the method described in the previous paragraph to compute the enrichment by counting each site with its posterior probability of being under selection, rather than with a uniform weight of 1 as we did in the previous paragraph.

Computational inference of miRNA expression based on the mRNA IP data

We used a linear model to predict the IP enrichment of a transcript in terms of the number of binding sites that it has for individual miRNAs, as well as of a factor reflecting the ''concentration'' of the miRNA in the cell. The miRNAs to be considered were determined based on published miRNA expression data (Landgraf et al. 2007). From this data set we extracted the list of miRNA seeds (nucleotides 1–8) that accumulated at least 50 sequences cloned from all the sampled tissues. We considered these 133 unique seeds for relating the enrichment in the IP to the miRNA expression.

The enrichment in the IP was measured, the number of binding sites for individual miRNAs in each 3′ UTR was calculated as the number of matches to positions 1–7, 2–8, or 1–8 of the miRNA, and using Matlab we fitted the weights w_m corresponding to all miRNAs in the expressions $E_i = \sum_{m \in \text{miRNAs}} w_m N_{i,m}$. Here, E_i is the logarithm of the fold change of transcript i in the IP compared with lysate, and $N_{i,m}$ is the number of sites for miRNA m in the 3′ UTR of transcript i. We then compared these weights with the relative miRNA frequencies measured by 454 sequencing, and we obtained a Pearson correlation coefficient of 0.37. Similarly, we correlated the inferred weights with the miRNA concentrations measured in a variety of other samples from Landgraf et al. (2007).

SUPPLEMENTAL DATA

Supplemental material can be found at http://www.rnajournal.org.

ACKNOWLEDGMENTS

We are grateful to Haiteng Deng and Joseph Fernandenz (Rockefeller University Proteomics Resource Facility) for the MS analysis, Wenxiang Zhang and Connie Zhao (Genomics Resource Center) for mRNA array analysis, and the Memorial Sloan Kettering Sequencing Core for 454 sequencing. We thank Jean Hausser for sharing some of his programs and Manuel Ascano, Thalia Farazi, Stefan Juranek, and other members of the laboratory for comments on the manuscript. We also thank Millipore for antibodies. D.G. was supported by Swiss National Fund grant #3100A0-114001 to M.Z. M.L. was supported by an Irma T. Hirschl Postdoctoral Fellowship. T.T. is an HHMI investigator, and work in his laboratory was supported by NIH grants GM073047 and GM068476.

Received September 5, 2008; accepted September 15, 2008.

REFERENCES

Ambros, V. 2004. The functions of animal microRNAs. *Nature* **431:** 350–355.

Baek, D., Villen, J., Shin, C., Camargo, F.D., Gygi, S.P., and Bartel, D.P. 2008. The impact of microRNAs on protein output. *Nature* **455:** 64–71.

Bagga, S., Bracht, J., Hunter, S., Massirer, K., Holtz, J., Eachus, R., and Pasquinelli, A.E. 2005. Regulation by *let-7* and *lin-4* miRNAs results in target mRNA degradation. *Cell* **122:** 553–563.

Balzer, E. and Moss, E.G. 2007. Localization of the developmental timing regulator Lin28 to mRNP complexes, P-bodies and stress granules. *RNA Biol.* **4:** 16–25.

Barth, S., Pfuhl, T., Mamiani, A., Ehses, C., Roemer, K., Kremmer, E., Jaker, C., Hock, J., Meister, G., and Grasser, F.A. 2008. Epstein-Barr virus-encoded microRNA miR-BART2 down-regulates the viral DNA polymerase BALF5. *Nucleic Acids Res.* **36:** 666–675.

Behm-Ansmant, I., Rehwinkel, J., Doerks, T., Stark, A., Bork, P., and Izaurralde, E. 2006. mRNA degradation by miRNAs and GW182 requires both CCR4:NOT deadenylase and DCP1:DCP2 decapping complexes. *Genes & Dev.* **20:** 1885–1898.

Beitzinger, M., Peters, L., Zhu, J.Y., Kremmer, E., and Meister, G. 2007. Identification of human microRNA targets from isolated argonaute protein complexes. *RNA Biol.* **4:** 76–84.

Bernstein, E., Caudy, A.A., Hammond, S.M., and Hannon, G.J. 2001. Role for a bidentate ribonuclease in the initiation step of RNA interference. *Nature* **409:** 363–366.

Bhattacharyya, S.N., Habermacher, R., Martine, U., Closs, E.I., and Filipowicz, W. 2006. Relief of microRNA-mediated translational repression in human cells subjected to stress. *Cell* **125:** 1111–1124.

Bushati, N. and Cohen, S.M. 2007. microRNA Functions. *Annu. Rev. Cell Dev. Biol.* **23:** 175–205.

Chapman, E.J. and Carrington, J.C. 2007. Specialization and evolution of endogenous small RNA pathways. *Nat. Rev. Genet.* **8:** 884–896.

Chendrimada, T.P., Gregory, R.I., Kumaraswamy, E., Norman, J., Cooch, N., Nishikura, K., and Shiekhattar, R. 2005. TRBP recruits the Dicer complex to Ago2 for microRNA processing and gene silencing. *Nature* **436:** 740–744.

Chu, C.Y. and Rana, T.M. 2006. Translation repression in human cells by microRNA-induced gene silencing requires RCK/p54. *PLoS Biol.* **4:** e210. doi: 10.1371/journal.pbio.0040210.

Denli, A.M., Tops, B.B., Plasterk, R.H., Ketting, R.F., and Hannon, G.J. 2004. Protein and RNA Composition of human AGO protein complexes processing of primary microRNAs by the Microprocessor complex. *Nature* **432:** 231–235.

Didiano, D. and Hobert, O. 2006. Perfect seed pairing is not a generally reliable predictor for miRNA-target interactions. *Nat. Struct. Mol. Biol.* **13:** 849–851.

Doench, J.G. and Sharp, P.A. 2004. Specificity of microRNA target selection in translational repression. *Genes & Dev.* **18:** 504–511.

Easow, G., Teleman, A.A., and Cohen, S.M. 2007. Isolation of microRNA targets by miRNP immunopurification. *RNA* **13:** 1198–1204.

Eulalio, A., Huntzinger, E., and Izaurralde, E. 2008. GW182 interaction with Argonaute is essential for miRNA-mediated translational repression and mRNA decay. *Nat. Struct. Mol. Biol.* **15:** 346–353.

Gaidatzis, D., van Nimwegen, E., Hausser, J., and Zavolan, M. 2007. Inference of miRNA targets using evolutionary conservation and pathway analysis. *BMC Bioinformatics* **8:** 69. doi: 10.1186/1471-2105-8-69.

Gentleman, R.C., Carey, V.J., Bates, D.M., Bolstad, B., Dettling, M., Dudoit, S., Ellis, B., Gautier, L., Ge, Y., Gentry, J., et al. 2004. Bioconductor: Open software development for computational biology and bioinformatics. *Genome Biol.* **5:** R80. doi: 10.1186/gb-2004-5-10-r89.

Giraldez, A.J., Mishima, Y., Rihel, J., Grocock, R.J., Van Dongen, S., Inoue, K., Enright, A.J., and Schier, A.F. 2006. Zebrafish MiR-430 promotes deadenylation and clearance of maternal mRNAs. *Science* **312:** 75–79.

Gregory, R.I., Yan, K.P., Amuthan, G., Chendrimada, T., Doratotaj, B., Cooch, N., and Shiekhattar, R. 2004. The microprocessor complex mediates the genesis of microRNAs. *Nature* **432:** 235–240.

Grimson, A., Farh, K.K., Johnston, W.K., Garrett-Engele, P., Lim, L.P., and Bartel, D.P. 2007. MicroRNA targeting specificity in mammals: Determinants beyond seed pairing. *Mol. Cell* **27:** 91–105.

Grishok, A., Pasquinelli, A.E., Conte, D., Li, N., Parrish, S., Ha, I., Baillie, D.L., Fire, A., Ruvkun, G., and Mello, C.C. 2001. Genes and mechanisms related to RNA interference regulate expression of the small temporal RNAs that control *C. elegans* developmental timing. *Cell* **106:** 23–34.

Grun, D., Wang, Y.L., Langenberger, D., Gunsalus, K.C., and Rajewsky, N. 2005. microRNA target predictions across seven *Drosophila* species and comparison to mammalian targets. *PLoS Comput. Biol.* **1:** e13. doi: 10.1371/journal.pcbi.0010013.

Haase, A.D., Jaskiewicz, L., Zhang, H., Laine, S., Sack, R., Gatignol, A., and Filipowicz, W. 2005. TRBP, a regulator of cellular PKR and HIV-1 virus expression, interacts with Dicer and functions in RNA silencing. *EMBO Rep.* **6:** 961–967.

Hammond, S.M., Boettcher, S., Caudy, A.A., Kobayashi, R., and Hannon, G.J. 2001. Argonaute2, a link between genetic and biochemical analyses of RNAi. *Science* **293:** 1146–1150.

Han, J., Lee, Y., Yeom, K.H., Kim, Y.K., Jin, H., and Kim, V.N. 2004. The Drosha–DGCR8 complex in primary microRNA processing. *Genes & Dev.* **18:** 3016–3027.

Han, J., Lee, Y., Yeom, K.H., Nam, J.W., Heo, I., Rhee, J.K., Sohn, S.Y., Cho, Y., Zhang, B.T., and Kim, V.N. 2006. Molecular basis for the recognition of primary microRNAs by the Drosha-DGCR8 complex. *Cell* **125:** 887–901.

Hendrickson, D.G., Hogan, D.J., Herschlag, D., Ferrell, J.E., and Brown, P.O. 2008. Systematic identification of mRNAs recruited to argonaute 2 by specific microRNAs and corresponding changes in transcript abundance. *PLoS One* **3:** e2126. doi: 10.1371/journal.pone.0002126.

Hock, J., Weinmann, L., Ender, C., Rudel, S., Kremmer, E., Raabe, M., Urlaub, H., and Meister, G. 2007. Proteomic and functional analysis of Argonaute-containing mRNA-protein complexes in human cells. *EMBO Rep.* **8:** 1052–1060.

Humphreys, D.T., Westman, B.J., Martin, D.I., and Preiss, T. 2005. MicroRNAs control translation initiation by inhibiting eukaryotic initiation factor 4E/cap and poly(A) tail function. *Proc. Natl. Acad. Sci.* **102:** 16961–16966.

Hutvágner, G. and Zamore, P.D. 2002. A microRNA in a multiple-turnover RNAi enzyme complex. *Science* **297:** 2056–2060.

Hutvágner, G., McLachlan, J., Bálint, É., Tuschl, T., and Zamore, P.D. 2001. A cellular function for the RNA interference enzyme Dicer in small temporal RNA maturation. *Science* **93:** 834–838.

Jakymiw, A., Lian, S., Eystathioy, T., Li, S., Satoh, M., Hamel, J.C., Fritzler, M.J., and Chan, E.K. 2005. Disruption of GW bodies impairs mammalian RNA interference. *Nat. Cell Biol.* **7:** 1267–1274.

Jing, Q., Huang, S., Guth, S., Zarubin, T., Motoyama, A., Chen, J., Di Padova, F., Lin, S.C., Gram, H., and Han, J. 2005. Involvement of microRNA in AU-rich element-mediated mRNA instability. *Cell* **120:** 623–634.

John, B., Enright, A.J., Aravin, A., Tuschl, T., Sander, C., and Marks, D. 2004. Human miRNA targets. *PLoS Biol.* **2:** e363. doi: 10.1371/journal.pbio.0020363.

Jones-Rhoades, M.W., Bartel, D.P., and Bartel, B. 2006. MicroRNAS and their regulatory roles in plants. *Annu. Rev. Plant Biol.* **57:** 19–53.

Karginov, F.V., Conaco, C., Xuan, Z., Schmidt, B.H., Parker, J.S., Mandel, G., and Hannon, G.J. 2007. A biochemical approach to identifying microRNA targets. *Proc. Natl. Acad. Sci.* **104:** 19291–19296.

Kedde, M., Strasser, M.J., Boldajipour, B., Vrielink, J.A., Slanchev, K., le Sage, C., Nagel, R., Voorhoeve, P.M., van Duijse, J., Orom, U.A., et al. 2007. RNA-binding protein Dnd1 inhibits microRNA access to target mRNA. *Cell* **131:** 1273–1286.

Ketting, R.F., Fischer, S.E., Bernstein, E., Sijen, T., Hannon, G.J., and Plasterk, R.H. 2001. Dicer functions in RNA interference and in synthesis of small RNA involved in developmental timing in *C. elegans*. *Genes & Dev.* **15:** 2654–2659.

Khvorova, A., Reynolds, A., and Jayasena, S.D. 2003. Functional siRNAs and miRNAs exhibit strand bias. *Cell* **115:** 209–216.

Kim, J., Krichevsky, A., Grad, Y., Hayes, G.D., Kosik, K.S., Church, G.M., and Ruvkun, G. 2004. Identification of many microRNAs that copurify with polyribosomes in mammalian neurons. *Proc. Natl. Acad. Sci.* **101:** 360–365.

Krek, A., Grun, D., Poy, M.N., Wolf, R., Rosenberg, L., Epstein, E.J., MacMenamin, P., da Piedade, I., Gunsalus, K.C., Stoffel, M., et al. 2005. Combinatorial microRNA target predictions. *Nat. Genet.* **37:** 495–500.

Krutzfeldt, J., Rajewsky, N., Braich, R., Rajeev, K.G., Tuschl, T., Manoharan, M., and Stoffel, M. 2005. Silencing of microRNAs in vivo with ''antagomirs.''. *Nature* **438:** 685–689.

Landgraf, P., Rusu, M., Sheridan, R., Sewer, A., Iovino, N., Aravin, A., Pfeffer, S., Rice, A., Kamphorst, A.O., Landthaler, M., et al. 2007. A mammalian microRNA expression atlas based on small RNA library sequencing. *Cell* **129:** 1401–1414.

Landthaler, M., Yalcin, A., and Tuschl, T. 2004. The human DiGeorge syndrome critical region gene 8 and Its *D. melanogaster* homolog are required for miRNA biogenesis. *Curr. Biol.* **14:** 2162–2167.

Lee, Y., Han, J., Yeom, K.H., Jin, H., and Kim, V.N. 2006a. Drosha in primary microRNA processing. *Cold Spring Harb. Symp. Quant. Biol.* **71:** 51–57.

Lee, Y., Hur, I., Park, S.Y., Kim, Y.K., Suh, M.R., and Kim, V.N. 2006b. The role of PACT in the RNA silencing pathway. *EMBO J.* **25:** 522–532.

Leung, A.K. and Sharp, P.A. 2007. microRNAs: A safeguard against turmoil? *Cell* **130:** 581–585.

Lewis, B.P., Burge, C.B., and Bartel, D.P. 2005. Conserved seed pairing, often flanked by adenosines, indicates that thousands of human genes are microRNA targets. *Cell* **120:** 15–20.

Lim, L.P., Lau, N.C., Garrett-Engele, P., Grimson, A., Schelter, J.M., Castle, J., Bartel, D.P., Linsley, P.S., and Johnson, J.M. 2005. Microarray analysis shows that some microRNAs down-regulate large numbers of target mRNAs. *Nature* **433:** 769–773.

Lingel, A., Simon, B., Izaurralde, E., and Sattler, M. 2004. Nucleic acid 3′-end recognition by the Argonaute2 PAZ domain. *Nat. Struct. Mol. Biol.* **11:** 576–577.

Linsley, P.S., Schelter, J., Burchard, J., Kibukawa, M., Martin, M.M., Bartz, S.R., Johnson, J.M., Cummins, J.M., Raymond, C.K., Dai, H., et al. 2007. Transcripts targeted by the microRNA-16 family cooperatively regulate cell cycle progression. *Mol. Cell. Biol.* **27:** 2240–2252.

Liu, J., Carmell, M.A., Rivas, F.V., Marsden, C.G., Thomson, J.M., Song, J.J., Hammond, S.M., Joshua-Tor, L., and Hannon, G.J. 2004. Argonaute2 is the catalytic engine of mammalian RNAi. *Science* **305:** 1437–1441.

Liu, J., Rivas, F.V., Wohlschlegel, J., Yates 3rd, J.R., Parker, R., and Hannon, G.J. 2005. A role for the P-body component GW182 in microRNA function. *Nat. Cell Biol.* **7:** 1261–1266.

Lund, E., Guttinger, S., Calado, A., Dahlberg, J.E., and Kutay, U. 2004. Nuclear export of microRNA precursors. *Science* **303:** 95–98.

Ma, J.B., Ye, K., and Patel, D.J. 2004. Structural basis for overhang-specific small interfering RNA recognition by the PAZ domain. *Nature* **429:** 318–322.

Ma, J.B., Yuan, Y.R., Meister, G., Pei, Y., Tuschl, T., and Patel, D.J. 2005. Structural basis for 5′-end-specific recognition of guide RNA by the *A. fulgidus* Piwi protein. *Nature* **434:** 666–670.

MacRae, I.J., Ma, E., Zhou, M., Robinson, C.V., and Doudna, J.A. 2008. In vitro reconstitution of the human RISC-loading complex. *Proc. Natl. Acad. Sci.* **105:** 512–517.

Maroney, P.A., Yu, Y., Fisher, J., and Nilsen, T.W. 2006. Evidence that microRNAs are associated with translating messenger RNAs in human cells. *Nat. Struct. Mol. Biol.* **13:** 1102–1107.

Martinez, J., Patkaniowska, A., Urlaub, H., Lührmann, R., and Tuschl, T. 2002. Single-stranded antisense siRNAs guide target RNA cleavage in RNAi. *Cell* **110:** 563–574.

Meister, G. and Tuschl, T. 2004. Mechanisms of gene silencing by double-stranded RNA. *Nature* **431:** 343–349.

Meister, G., Landthaler, M., Patkaniowska, A., Dorsett, Y., Teng, G., and Tuschl, T. 2004. Human Argonaute2 mediates RNA cleavage targeted by miRNAs and siRNAs. *Mol. Cell* **15:** 185–197.

Meister, G., Landthaler, M., Peters, L., Chen, P.Y., Urlaub, H., Luhrmann, R., and Tuschl, T. 2005. Identification of novel argonaute-associated proteins. *Curr. Biol.* **15:** 2149–2155.

Mourelatos, Z., Dostie, J., Paushkin, S., Sharma, A., Charroux, B., Abel, L., Rappsilber, J., Mann, M., and Dreyfuss, G. 2002. miRNPs: A novel class of ribonucleoproteins containing numerous microRNAs. *Genes & Dev.* **16:** 720–728.

Nelson, P.T., Hatzigeorgiou, A.G., and Mourelatos, Z. 2004. miRNP:mRNA association in polyribosomes in a human neuronal cell line. *RNA* **10:** 387–394.

Nottrott, S., Simard, M.J., and Richter, J.D. 2006. Human let-7a miRNA blocks protein production on actively translating polyribosomes. *Nat. Struct. Mol. Biol.* **13:** 1108–1114.

Olsen, P.H. and Ambros, V. 1999. The lin-4 regulatory RNA controls developmental timing in *Caenorhabditis elegans* by blocking LIN-14 protein synthesis after the initiation of translation. *Dev. Biol.* **216:** 671–680.

Orom, U.A. and Lund, A.H. 2007. Isolation of microRNA targets using biotinylated synthetic microRNAs. *Methods* **43:** 162–165.

Parker, J.S., Roe, S.M., and Barford, D. 2005. Structural insights into mRNA recognition from a PIWI domain-siRNA guide complex. *Nature* **434:** 663–666.

Patel, D.J., Ma, J.B., Yuan, Y.R., Ye, K., Pei, Y., Kuryavyi, V., Malinina, L., Meister, G., and Tuschl, T. 2006. Structural biology of RNA silencing and its functional implications. *Cold Spring Harb. Symp. Quant. Biol.* **71:** 81–93.

Pellino, J.L., Jaskiewicz, L., Filipowicz, W., and Sontheimer, E.J. 2005. ATP modulates siRNA interactions with an endogenous human Dicer complex. *RNA* **11:** 1719–1724.

Peters, L. and Meister, G. 2007. Argonaute proteins: Mediators of RNA silencing. *Mol. Cell* **26:** 611–623.

Petersen, C.P., Bordeleau, M.E., Pelletier, J., and Sharp, P.A. 2006. Short RNAs repress translation after initiation in mammalian cells. *Mol. Cell* **21:** 533–542.

Pham, J.W., Pellino, J.L., Lee, Y.S., Carthew, R.W., and Sontheimer, E.J. 2004. A Dicer-2-dependent 80s complex cleaves targeted mRNAs during RNAi in *Drosophila*. *Cell* **117:** 83–94.

Pillai, R.S., Bhattacharyya, S.N., Artus, C.G., Zoller, T., Cougot, N., Basyuk, E., Bertrand, E., and Filipowicz, W. 2005. Inhibition of translational initiation by Let-7 microRNA in human cells. *Science* **309:** 1573–1576.

Rajewsky, N. 2006. microRNA target predictions in animals. *Nat. Genet.* (Suppl) **38:** S8–S13.

Rehwinkel, J., Behm-Ansmant, I., Gatfield, D., and Izaurralde, E. 2005. A crucial role for GW182 and the DCP1:DCP2 decapping complex in miRNA-mediated gene silencing. *RNA* **11:** 1640–1647.

Rehwinkel, J., Natalin, P., Stark, A., Brennecke, J., Cohen, S.M., and Izaurralde, E. 2006. Genome-wide analysis of mRNAs regulated by Drosha and Argonaute proteins in *Drosophila melanogaster*. *Mol. Cell. Biol.* **26:** 2965–2975.

Robb, G.B. and Rana, T.M. 2007. RNA helicase A interacts with RISC in human cells and functions in RISC loading. *Mol. Cell* **26:** 523–537.

Rodriguez, A., Vigorito, E., Clare, S., Warren, M.V., Couttet, P., Soond, D.R., van Dongen, S., Grocock, R.J., Das, P.P., Miska, E.A., et al. 2007. Requirement of bic/microRNA-155 for normal immune function. *Science* **316:** 608–611.

Schmitter, D., Filkowski, J., Sewer, A., Pillai, R.S., Oakeley, E.J., Zavolan, M., Svoboda, P., and Filipowicz, W. 2006. Effects of Dicer and Argonaute down-regulation on mRNA levels in human HEK293 cells. *Nucleic Acids Res.* **34:** 4801–4815.

Schwarz, D.S., Hutvágner, G., Du, T., Xu, Z., Aronin, N., and Zamore, P.D. 2003. Asymmetry in the assembly of the RNAi enzyme complex. *Cell* **115:** 199–208.

Seggerson, K., Tang, L., and Moss, E.G. 2002. Two genetic circuits repress the *Caenorhabditis elegans* heterochronic gene *lin-28* after translation initiation. *Dev. Biol.* **243:** 215–225.

Selbach, M., Schwanhausser, B., Thierfelder, N., Fang, Z., Khanin, R., and Rajewsky, N. 2008. Widespread changes in protein synthesis induced by microRNAs. *Nature* **455:** 58–63.

Song, J.J., Liu, J., Tolia, N.H., Schneiderman, J., Smith, S.K., Martienssen, R.A., Hannon, G.J., and Joshua-Tor, L. 2003. The crystal structure of the Argonaute2 PAZ domain reveals an RNA binding motif in RNAi effector complexes. *Nat. Struct. Biol.* **10:** 1026–1032.

Song, J.J., Smith, S.K., Hannon, G.J., and Joshua-Tor, L. 2004. Crystal structure of Argonaute and its implications for RISC slicer activity. *Science* **305:** 1434–1437.

Thermann, R. and Hentze, M.W. 2007. *Drosophila* miR2 induces pseudo-polysomes and inhibits translation initiation. *Nature* **447:** 875–878.

Tolia, N.H. and Joshua-Tor, L. 2007. Slicer and the argonautes. *Nat. Chem. Biol.* **3:** 36–43.

Vasudevan, S. and Steitz, J.A. 2007. AU-rich-element-mediated upregulation of translation by FXR1 and Argonaute 2. *Cell* **128:** 1105–1118.

Vasudevan, S., Tong, Y., and Steitz, J.A. 2007. Switching from repression to activation: MicroRNAs can up-regulate translation. *Science* **318:** 1931–1934.

Vinther, J., Hedegaard, M.M., Gardner, P.P., Andersen, J.S., and Arctander, P. 2006. Identification of miRNA targets with stable isotope labeling by amino acids in cell culture. *Nucleic Acids Res.* **34:** e107.

Wakiyama, M., Takimoto, K., Ohara, O., and Yokoyama, S. 2007. Let-7 microRNA-mediated mRNA deadenylation and translational repression in a mammalian cell-free system. *Genes & Dev.* **21:** 1857–1862.

Wightman, B., Ha, I., and Ruvkun, G. 1993. Posttranscriptional regulation of the heterochronic gene *lin-14* by *lin-4* mediates temporal pattern formation in *C. elegans*. *Cell* **75:** 855–862.

Wu, L., Fan, J., and Belasco, J.G. 2006. MicroRNAs direct rapid deadenylation of mRNA. *Proc. Natl. Acad. Sci.* **103:** 4034–4039.

Wu, Z., Irizarry, R.A., Gentleman, R., Martinez-Murillo, F., and Spencer, F. 2004. A model-based background adjustment for oligonucleotide expression arrays. *J. Am. Stat. Assoc.* **99:** 909–917.

Yan, K.S., Yan, S., Farooq, A., Han, A., Zeng, L., and Zhou, M.M. 2003. Structure and conserved RNA binding of the PAZ domain. *Nature* **426:** 468–474.

Yekta, S., Shih, I.H., and Bartel, D.P. 2004. MicroRNA-directed cleavage of HOXB8 mRNA. *Science* **304:** 594–596.

Yi, R., Qin, Y., Macara, I.G., and Cullen, B.R. 2003. Exportin-5 mediates the nuclear export of pre-microRNAs and short hairpin RNAs. *Genes & Dev.* **17:** 3011–3016.

Yisraeli, J.K. 2005. VICKZ proteins: A multi-talented family of regulatory RNA-binding proteins. *Biol. Cell* **97:** 87–96.

Zeng, Y., Wagner, E.J., and Cullen, B.R. 2002. Both natural and designed microRNAs can inhibit the expression of cognate mRNAs when expressed in human cells. *Mol. Cell* **9:** 1327–1333.

Zhang, L., Ding, L., Cheung, T.H., Dong, M.Q., Chen, J., Sewell, A.K., Liu, X., Yates 3rd, J.R., and Han, M. 2007. Systematic identification of *C. elegans* miRISC proteins, miRNAs, and mRNA targets by their interactions with GW182 proteins AIN-1 and AIN-2. *Mol. Cell* **28:** 598–613.

Zhao, Y., Ransom, J.F., Li, A., Vedantham, V., von Drehle, M., Muth, A.N., Tsuchihashi, T., McManus, M.T., Schwartz, R.J., and Srivastava, D. 2007. Dysregulation of cardiogenesis, cardiac conduction, and cell cycle in mice lacking miRNA-1-2. *Cell* **129:** 303–317.